New complexes and materials for O$_2$-based oxidations

Craig L. Hill[*], Travis M. Anderson, Jong Woo Han, Daniel A. Hillesheim, Yurii V. Geletii,
Nelya M. Okun, Rui Cao, Bogdan Botar, Djamaladdin G. Musaev, Keiji Morokuma

Department of Chemistry, Emory University, Atlanta, GA 30322, United States

Available online 27 March 2006

Abstract

Key experiments in three developing dioxygen activation and oxo transfer projects are described. First, the Pt–oxo complex, $K_7Na_9Pt^{IV}$ $(O)(OH_2)(PW_9O_{34})_2$ (KNa**1**) is further addressed and its first reactivity is noted (oxo transfer under Ar at ambient temperature to PPh$_3$ forming O=PPh$_3$ with nearly quantitative selectivity). Second, an unusually reactive catalyst for aerobic oxygenation of sulfides to sulfoxides (TBANO$_3$ in the presence of TBA$_4$Fe(H$_2$O)PW$_{11}$O$_{39}$ in acetonitrile solvent) is reported and its stoichiometry is established to be the desired atom-efficient dioxygenase one (RSR + $(1/2)O_2 \rightarrow$ RS(O)R). Third, a crystalline microporous solid (metal organic framework material) capable of catalyzing air-based oxidations is described. Reaction of the bis(triesterified)hexavanadate unit terminating in two carboxylate functions, $[(n-C_4H_9)_4N]_2[V_6O_{13}\{(CH_2O)_3CNHCH_2(4-C_6H_4COOH)\}_2]$ reacts with Co(NO$_3$)$_2$·6H$_2$O and 4,4′-bipyridine to form a ladder-like microporous polymer, characterized by X-ray crystallography, that catalyzes the air-based oxidation of a representative thiol, *n*-PrSH, cleanly to the corresponding disulfide, PrSSPr. The esterified hexavanadate units are the catalysts, and there is no reaction in the absence of the microporous material.

1. Introduction

Catalytic systems for O$_2$-based oxidations under mild conditions remain of considerable intellectual and practical interest [1–5]. Those that function with air under ambient conditions are even more problematical to design and realize but have potential value not only in selective homogeneous catalytic oxidation (production of specialty chemicals, etc.) but also in nascent technologies including coatings, fabrics and other materials that catalyze air-based oxidative removal or decontamination of air pollutants, chemical warfare agents and other undesirable species [6,7].

In this context, we report here results from three emerging efforts in our research group that address the longstanding and ongoing challenge of O$_2$-based oxidation from a different perspective. First, a Pt–oxo complex recently described, the initial example of a high-d-electron-count terminal metal–oxo complex, [8] is now shown to transfer oxygen (derived from O$_2$) into organic substrates. Second, highly reactive complexes for

air-based sulfoxidation using the ambient environment (1 atm of air at room temperature), which were also recently reported, [9] are now shown to undergo reactions proceeding by the desired atom-efficient dioxygenase stoichiometry. Third, long-sought crystalline microporous materials with the ability to catalyze oxidations under ambient conditions are presented (for the first time).

2. Experimental section

2.1. Materials and methods

TBANO$_3$, *p*-toluenesulphonic acid (pTSH), 2-chloroethyl ethyl sulfide (CEES), chloromethyl benzoic acid, tris(hydroxymethyl)aminomethane, 1-propanethiol, decane, 1,3-dichlorobenzene, triphenylphosphine and triphenylphosphine oxide were commercially available samples. α-Na$_7$PW$_{11}$O$_{39}$, [10] Na$_4$Fe(H$_2$O)PW$_{11}$O$_{39}$, [11] [(*n*-C$_4$H$_9$)$_4$N]$_2$[H$_3$V$_{10}$O$_{28}$], [12] and A-α-Na$_8$HPW$_9$O$_{34}$ [13] were prepared and purified by literature procedures. TBA$_4$Fe(H$_2$O)PW$_{11}$O$_{39}$·nH$_2$O was prepared by adding TBABr to an aqueous solution of [Fe(H$_2$O)PW$_{11}$O$_{39}$]$^{4-}$ and collecting the resulting precipitate.

---
[*] Corresponding author. Tel.: +1 404 727 6611; fax: +1 404 727 6076.
E-mail address: chill@emory.edu (C.L. Hill).

Elemental analyses were performed by Atlantic Microlab Inc. (Norcross, Georgia), Kanti Labs (Mississauga, Canada), Quantitative Technologies Inc. (Whitehouse, New Jersey), and Desert Analytics (Tucson, Arizona). Infrared (2% sample in KBr) and Raman spectra were recorded on a Thermo Nicolet 6700 instrument. The electronic absorption spectra were taken on a Hewlett–Packard 8452A UV–vis spectrophotometer. ^{1}H and ^{31}P NMR measurements were made on a Varian INOVA 400 MHz spectrometer, and ^{51}V NMR measurements were made on a Varian Unity 600 MHz spectrometer. Oxidation reactions were quantified by gas chromatography (GC; Hewlett Packard 5890 series gas chromatograph equiped with a flame ionization detector, 5% phenyl methyl silicone capillary column, N_2 carrier gas, and a Hewlett Packard 3390A series integrator). Consumption of oxygen was monitored using an Artisan RS-232 digital manometer. Differential scanning calorimetric and thermogravimetric data were collected on Instrument Specialists Incorporated DSC 550 and TGA 1000 instruments, respectively.

2.2. Synthesis and characterization of $K_7Na_9Pt^{IV}(O)(OH_2)(PW_9O_{34})_2 \cdot 21.5H_2O$ (KNa**1**)

A 1.0-g (2.4 mmol) sample of potassium tetrachloroplatinate (K_2PtCl_4) was dissolved in 200 mL of deionized water at room temperature (pH = 4) and 3.6 g (1.42 mmol) of freshly prepared A-α-$Na_8HPW_9O_{34}$ was added quickly with vigorous stirring of the solution. The mixture was stirred until a nearly clear pink solution was obtained (ca. 2 min) (pH = 7), and then filtered with a fine glass-sintered frit. A 20-g sample of KCl was added to the filtrate, the solution was stirred for an additional 2 min, and then it was filtered to obtain a white solid. The solid was dried in air overnight and then re-dissolved in a minimal amount of water with heating to 55 °C. The clear, colorless solution gradually turned to a deep yellow color over 3 days. Shortly after the appearance of the deep yellow color, large brown crystals of **1** (1 g, yield 25%) appeared along with a small amount of yellow–pink precipitate. The crystals were manually removed from the solution and washed with 5 °C water to remove any precipitate from the surface. IR (2% KBr pellet, 1300–400 cm^{-1}): 1072 (s), 1015 (m, sh), 940 (s), 833 (s), 746 (s), 612 (m), and 513 (w). ^{31}P NMR (9 mM solution in D_2O, referenced to 85% H_3PO_4): -8.8 ($\Delta\nu_{1/2} = 30$ Hz). Electronic spectral data (400–800 nm, in H_2O (6.14 mM sample, 1 cm cell path length)) [λ, nm (ε, M^{-1} cm^{-1})]: 428 nm (210), 502 (73) and 574 nm (43). Magnetic susceptibility: $\mu_{eff} = 0$ μ_B/mol at 297 K. Anal. Calcd. for $K_7Na_9Pt^{IV}(O)(OH_2)(PW_9O_{34})_2 \cdot 21.5H_2O$: K, 4.92; Na, 3.72; P, 1.11; Pt, 3.51; W, 59.47. Found: K, 4.87; Na, 3.66; P, 1.12; Pt, 3.71; W, 60.71. [MW = 5564 g/mol].

2.3. Stoichiometric oxidation of Ph_3P with **1**

A finely ground 0.2 g (0.036 mmol) sample of **1** was suspended in 1 mL of toluene, heptane, or acetonitrile. The apparatus was evacuated and refilled with Ar, and this cycle was repeated 10 times. A 8.5 mg sample of Ph_3P (0.032 mmol) was then added to this suspension and the reaction vessel was immediately sealed. The reaction was stirred at ambient temperature

for 24 h, and ^{31}P NMR and FT-IR was used to monitor the reaction.

2.4. Reactive catalyst for aerobic sulfide oxidation

A 25-mL round bottom flask with side arm was charged with TBANO$_3$ (0.0105 mmol), *p*-toluenesulfonic acid (0.0108 mmol), $TBA_4Fe(H_2O)PW_{11}O_{39}$ (0.0045 mmol), 1,3-dichlorobenzene (0.83 mmol), and 2-chloroethyl ethyl sulfide (CEES) (0.86 mmol). Dry acetonitrile was added to give a total volume of 5 mL. The apparatus was flushed with O_2 (total volume 40 mL) and equipped with a magnetic stir bar, gas tight septum, and a digital manometer, and the flask was placed in a water bath at room temperature.

2.5. Synthesis of $(4-C_6H_4COOH)CH_2NHC(CH_2OH)_3$ (acid–Tris)

Solid *p*-chloromethyl benzoic acid (10.0 g, 0.0586 mol) was added to a solution of tris(hydroxymethyl)aminomethane (35.6 g, 0.294 mol) in 300 mL of water over ca. 2-min period. The mixture was stirred for 20 h at room temperature. The chloromethyl benzoic acid was completely dissolved in 30 min, and a white precipitate began to appear about 7 h after the addition. The white precipitate was filtered and washed with water (2 mL × 20 mL) and acetone (2 mL × 15 mL) and dried under vacuum for 24 h to yield 10.2 g of product (68.0%). ^{1}H NMR (DMSO-d_6): 4.64 (d, 12H). Anal. Calcd. for $C_{12}H_{17}NO_5$: H, 6.23; C, 53.09; N, 12.38. Found: H, 6.13; C, 52.58; N, 12.13.

2.6. Synthesis $[(n-C_4H_9)_4N]_2[V_6O_{13}\{(CH_2O)_3CNHCH_2(4-C_6H_4COOH)\}_2]$ (TBA$_2$[H$_2$**4**])

Acid–Tris (6.00 g 23.5 mmol) and $[(n-C_4H_9)_4N]_3[H_3V_{10}O_{28}]$ (13.2 g, 7.83 mmol) were dissolved in 240 ml of dry dimethyl acetamide (DMA). The orange solution was stirred at 85 °C for 24 h under an O_2 atmosphere. The solution was cooled to room temperature and then 720 mL of diethyl ether was added. The sticky precipitate that formed was isolated by decanting solvent. A 120-mL aliquot of acetone was added, and the mixture was stirred for 1 h to obtain a powdered product. This product was filtered and washed with acetone (3 mL × 10 mL). The filtrate was concentrated to ca. 30 mL and left undisturbed for 6 h to obtain a powdered precipitate. The precipitate was filtered and washed with a small amount of acetone. This crude product was re-dissolved in 70 mL of a mixed solvent of acetonitrile and dimethyl formamide (DMF) (v/v = 1/1). A 150-mL aliquot of diethyl ether was added to precipitate the product. This product was filtered and washed with diethyl ether (2 mL × 10 mL) and purified by crystallization (acetonitrile/DMF/diethyl ether = 1/1/4) (6.01 g, 29.2% based on vanadium). ^{1}H NMR (DMSO-d_6): δ = 0.92 (t, 24H), 1.30 (sextet, 16H), 1.55 (quintet, 16H), 3.15 (t, 16H), 3.77 (s, 4H), 4.88 (d, 12H), 7.26 (d, 4H), 7.72 (d, 4H). ^{51}V NMR (DMSO-d_6): δ = -493.6. Anal. Calcd. for $C_{62}H_{114}N_6O_{25}V_6$

(TBA$_2$H$_2$**4**·2DMF): H, 6.97; C, 45.15; N, 5.10; V, 18.5. Found: H, 6.91; C, 44.97; N, 5.14; V, 18.2.

2.7. Synthesis of [Co$_2$Bpy$_2$(DMSO)$_2$ (DMF)$_2$(H$_2$O)$_2$**4**]·2.1DMF(Co**4**)

An 8.0 mL aliquot of Co(NO$_3$)$_2$·6H$_2$O dissolved in DMF (10 mM) was added to 4.0 mL of a 10 mM solution of TBA$_2$[H$_2$**4**] dissolved in DMF (10 mM) and 4.0 mL of 20 mM 4,4′-bipyridine (Bpy) dissolved in DMSO was slowly layered on top of the solution. The crystallization system was allowed to stand for 5 days without disturbance. The red crystals which form over this time period were filtered, washed with dichloroethane, and dried in a vacuum (40 mg yield). Anal. Calcd. for CoC$_{60}$H$_{78.7}$N$_{10.1}$O$_{29.1}$S$_2$V$_6$: H, 4.31; C, 39.38; N, 7.69; S, 3.49; V, 16.62; Co, 3.20. Found: H, 4.49; C, 34.00; N, 7.51; S, 3.4; V, 16.5; Co, 3.3. (IR (KBr, 400–4000 cm^{-1})): 3421 (s, br), 2923 (m), 2852 (m), 1705 (w), 1653 (s), 1622 (m), 1468 (w), 1411 (w), 1253 (m), 1185 (w), 1099 (s), 1027 (m), 962(s), 787 (s), 723 (m), 588 (w), 413 (m).

2.8. Aerobic oxidation of 1-propanethiol with Co**4**

In a typical experiment, 0.33 mmol (0.11 M) of 1-propanethiol (PrSH), 0.031 mmol (0.010 M) of decane (internal standard), and 0.0097 mmol (3.2 mM) of Co**4** were added to 2.9 mL of dichloroethane in a Schlenk flask fitted with a plug made of PTFE under air at 45 °C using a temperature-controlled water bath. Aliquots were removed over a period of 7 days and analyzed by GC.

2.9. Crystallographic studies of Co**4**

Suitable crystals of Co**4** were coated with Paratone N oil, suspended on a small fiber loop, and placed in a cooled nitrogen stream at 100 K on a Bruker D8 SMART APEX CCD sealed tube diffractometer with graphite monochromated Mo Kα (0.71073 Å) radiation. Redundant data were measured using a series of combinations of ϕ and ω scans with 10 s frame exposures and 0.3° frame widths. Data collection, indexing, and initial cell refinements were handled using SMART software (Version 5.624, Brüker AXS, Inc.). Frame integration and final cell refinements were carried out using SAINT software (Version 6.36A, Brüker AXS, Inc.). The final cell parameters were determined from least-squares refinements and the SADABS program (Version 2.10, George Sheldrick, University of Göttingen) was used to carry out absorption corrections. The structures were solved using Direct Methods and difference Fourier techniques. All non-hydrogen atoms were refined anisotropically, except for one of the disordered pyridine moieties of bipyridine. Only one solvent DMF molecule in the void space could be reasonably modeled. The high *R*-value reflects the large number of disordered and dynamic solvent molecules in the channels, a situation that is not uncommon for crystals of solvent-saturated highly porous materials. The final R_1 scattering factors and anomalous dispersion corrections were taken from the *International Tables for X-ray Crystallography* [14] (Table 1).

Table 1
Crystal data and structure refinement for Co**4**

Empirical formula	C$_{60.60}$H$_{82}$Co$_2$N$_{10.30}$O$_{31.30}$S$_2$V$_6$
Formula weight	1943.21
Temperature	173(2) K
Wavelength	0.71073 Å
Crystal system	Triclinic
Space group	$P\bar{1}$
Unit cell dimensions	$a = 11.4581(11)$ Å,
	$b = 11.4897(11)$ Å,
	$c = 19.1503(19)$ Å, $\alpha = 81.198(2)°$,
	$\beta = 76.619(2)°$, $\gamma = 81.716(2)°$
Volume	2408.3(4) Å^3
Z	1
Density (calculated)	1.340 g/cm^3
θ range for data collection	1.84–28.33°
Reflections collected	33452
Independent reflections	11977 [$R_{(int)} = 0.0703$]
Completeness to theta $= 28.33°$	99.6%
Data/restraints/parameters	11977/0/346
Goodness-of-fit on F^2	1.148
Final R indices [$I > 2\sigma(I)$]	$R_1 = 0.1076$, $wR_2 = 0.3249$
R indices (all data)	$R_1 = 0.1588$, $wR_2 = 0.3647$
Largest difference peak and hole	2.933 and −1.243e

3. Results and discussion

3.1. Synthesis, characterization, and stoichiometric oxo transfer studies of K$_7$Na$_9$Pt(O) (OH$_2$)(PW$_9$O$_{34}$)$_2$·21.5H$_2$O (KNa**1**)

Reaction of an aqueous solution of Pt(II) (from K$_2$PtCl$_4$) with the tri-tungsten-vacant POM, Na$_9$[A-α-PW$_9$O$_{34}$], followed by rapid precipitation with KCl, results in the formation of Na$_{16}$[Pt(PW$_9$O$_{34}$)$_2$] based on previous infrared and ^{31}P NMR spectroscopic measurements as well as elemental analysis data (i.e. the ratio of Na:P:Pt:W is 16:2:1:18) [8]. An aqueous solution of [Pt^{II}(PW$_9$O$_{34}$)$_{34}$]$^{16-}$ oxidizes to [Pt^{IV}(O)(OH$_2$) (PW$_9$O$_{34}$)$_2$]$^{16-}$ (**1**) during a 3-day exposure to air. The oxidation of **1** is immediately followed by crystallization, and the isolated compound is obtained in ~25% yield. An X-ray diffraction study (at 193 K) was previously performed on **1**, and the results reveal that a single Pt(IV) center is ligated by one terminal oxo unit, two bidentate symmetry-equivalent [A-α-PW$_9$O$_{34}$]$^{9-}$ clusters, and one aqua ligand *trans* to the terminal oxo [8].

Although an isostructural W(VI) analogue of **1** is known, there are several lines of evidence which indicate that **1** is not actually [W(O)(OH$_2$)(PW$_9$O$_{34}$)$_2$]$^{14-}$ (**2**). First the metal–terminal oxo bond distances are different for the two complexes (1.72 Å for **1** versus 1.67 Å for **2**). Second, the displacement of the central metal atoms from the O$_4$ equatorial planes (defined by the four oxygen atoms of the two [A-α-PW$_9$O$_{34}$]$^{9-}$ units and illustrated in Fig. 1A) of **1** and **2** are 0.31 and 0.45 Å, respectively. Finally, the elemental analysis data suggest that the ratio of P:Pt:W in **1** is exactly 2:1:18.

Low temperature X-ray studies at 30 K confirm that **2** is not actually a co-crystalline mixture of **1** and **2**. To establish the validity of this method for distinguishing co-crystalline mixtures, a Pd(II)–OH$_2$ complex, [Pd(H$_2$O)$_2$(PW$_9$O$_{34}$)$_2$]$^{16-}$ (**3**),
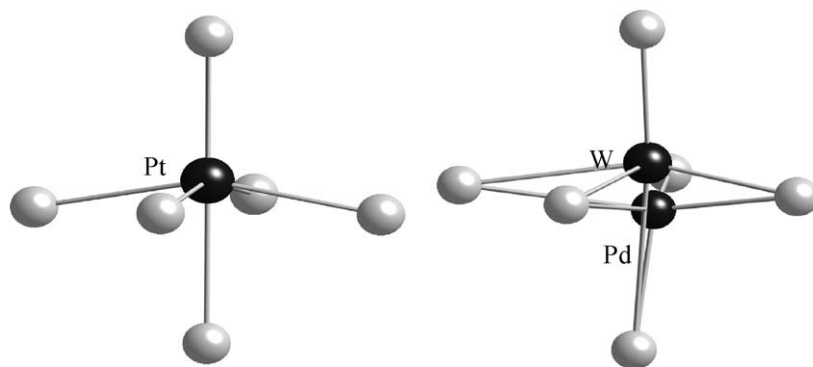
Fig. 1. Coordination environment of the Pt(IV) ion in **1** showing the characteristic out-of-plane displacement of a M=O moiety in terminal oxo complexes (left) and schematic representation of the coordination environment of the Pd(II) ion in a co-crystalline mixture of **2** and **3** (right).

structurally analogous to **1** and **2**, was prepared by a procedure similar to that for **1** except the pH was ~2 (to keep Pd(II) in solution), versus ~7 for **1**. The lower pH required to synthesize **3** causes **2** to form. Although **2** and **3** co-crystallize, a good X-ray structure ($R = 5.2\%$) of a crystal 70% **2** and 30% **3**, clearly distinguishes the positions of the central W(VI) and Pd(II) centers and the short (1.68 Å) W(VI)-oxo bond from the long (2.14 Å) Pd(II)-OH$_2$ bond (Fig. 1B).

Due to the low stability of **1**, it was not possible to screen this compound for catalytic activity. However, we now report that the mixed Na–K$^+$ salt of **1**, which is not soluble in heptane, acetonitrile, or toluene (i.e. each solvent tested individually), is an effective stoichiometric oxo transfer reagent. The insolubility of **1** is based on the absence of the intense oxygen-to-tungsten charge transfer bands (characteristic of **1** and almost all POMs in general) in the UV–vis spectra of a suspension of **1** in heptane, acetonitrile, or toluene. This heterogeneous system (i.e. insoluble powder suspended in either heptane, acetonitrile, or toluene) transfers oxygen to triphenylphosphine (to form exclusively triphenylphosphine oxide based on ^{31}P NMR data) with 100% conversion in 24 h at ambient temperature under Ar when **1** is present in slight excess relative to Ph$_3$P. A control experiment, performed under identical conditions, except that **1** was absent, yielded no triphenylphosphine oxide. In addition, the reaction was performed using **2** instead of **1** (again under identical conditions), and no triphenylphosphine oxide was formed.

3.2. A reactive catalyst for aerobic sulfide oxidation

As previously reported, a catalyst comprised of TBANO$_3$, pTSH, and TBA$_4$Fe(H$_2$O)PW$_{11}$O$_{39}$ (ca. 2:2:1 equivalents, respectively) in acetonitrile solution converts ~70% of the sulfide CEES (a mustard simulant) to the corresponding sulfoxide, CEESO, after 6 h reaction time with effectively 100% selectivity (no sulfone or other organic product is detected) [9]. This corresponds to ~150 turnovers with a TOF ~ 40 h^{-1}, a remarkably high value for oxidation using the ambient environment (air as the oxidant at room temperature). A key is to determine the stoichiometry from quantifying both consumption of CEES and O$_2$ simultaneous with production of CEESO. This was now done using gas chromatography (for CEES and CEESO) and quantitative manometry (for O$_2$). The moles of O$_2$ present were

determined from the ideal gas equation (with R adjusted to room temperature). At low conversion (and specifically with low quantities of CEESO), it was problematical to achieve mass balance. This appears to be a direct result of the fact that it is difficult to quantify CEESO by gas chromatography at very low conversions (concentrations). Nonetheless, the stoichiometry at higher conversions was clearly determined to the desired (atom-efficient) dioxygenase one: CEES + ⟨1/2⟩O$_2$ → CEESO (Fig. 2).

3.3. Synthesis, characterization, and catalytic reactivity of Co**4**

The zwitterionic triol derivative, (4-C$_6$H$_4$COOH)CH$_2$NHC(CH$_2$OH)$_3$ (acid–Tris), was prepared by the reaction of (HOCH$_2$)$_3$CNH$_2$ and chloromethyl benzoic acid in water for 20 h at 22 °C. The bis(benzoic acid) capped hexavanadate, [(n-C$_4$H$_9$)$_4$N]$_2$[V$_6$O$_{13}${(CH$_2$O)$_3$CNHCH$_2$(4-C$_6$H$_4$COOH)}$_2$] (TBA$_2$[H$_2$**4**]), was prepared by the reaction of acid–Tris with [(n-C$_4$H$_9$)$_4$N]$_3$[H$_3$V$_{10}$O$_{28}$] in DMA at 85 °C for 60 h under O$_2$, a modification of the method used by Zubieta and coworkers for the –CH$_3$, –CH$_2$CH$_3$, –NO$_2$ and –CH$_2$OH derivatives [15]. The combination of Co(NO$_3$)$_2$·6H$_2$O, 4,4′-bipyridine, and TBA$_2$[H$_2$**4**] in a DMSO/DMF (1/3 = v/v) mixed solvent
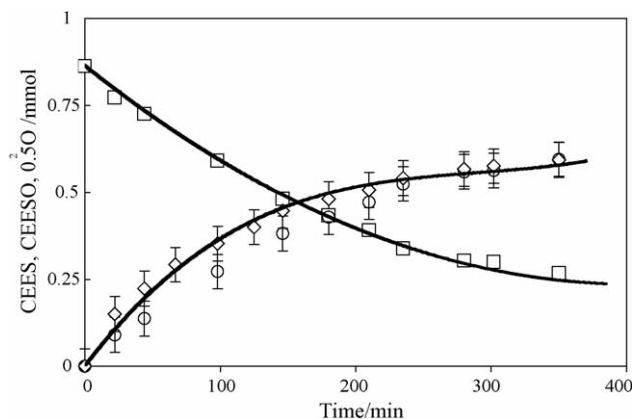
Fig. 2. Oxidation of CEES to CEESO catalyzed by the nitrate (4 mM TBANO$_3$)/proton (2 mM pTSH)/TBA$_4$Fe(H$_2$O)PW$_{11}$O$_{39}$ (0.8 mM) system in acetonitrile (5 mL) at 25 °C and 1 atm O$_2$. The squares represent CEES, the circles represent CEESO, and the diamonds represent O$_2$.
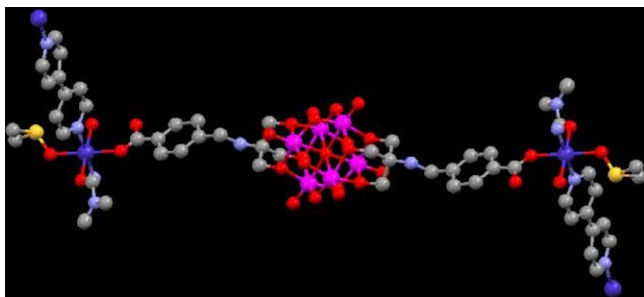
Fig. 3. Coordination environment of the Co(II) center in Co**4**. The hydrogen atoms have been omitted for clarity.
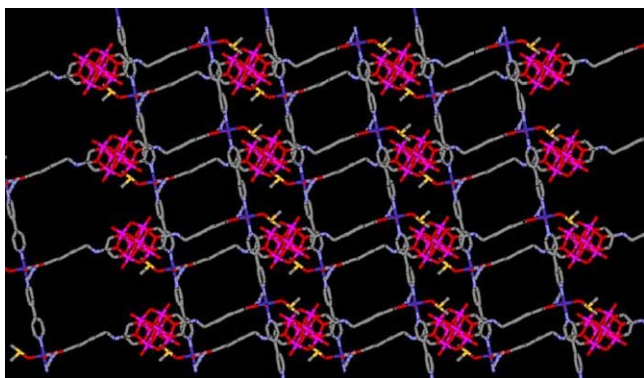

Fig. 4. A view parallel to the [0 1 0] plane of the crystal of Co**4**. The hydrogen atoms and the solvent DMF molecules occupying the void space have been omitted for clarity.

produced a ladder-type coordination network material Co**4**, regardless of the ratio of the reactants. The Co(II) center is six coordinate with 1 DMSO, 1 DMF, 1 water, 1 benzoic acid, and 2 bpy ligands, which are *trans* to each other. This coordination unit from the single crystal X-ray structure is shown in Fig. 3. The aqua ligand coordinated to Co(II) is hydrogen bonding to the carbonyl group of the benzoic acid moiety, which is also coordinated to the Co(II) center. Two coordination chains formed by Co(II) and bpy are connected by a unit of **4** to form a microporous ladder-type coordination network (Fig. 4).

The catalytic activity of Co**4** was evaluated in dichloroethane, a solvent in which this coordination polymer is totally insoluble. Co**4** catalyzes the aerobic oxidation of PrSH to its corresponding disulfide product, PrSSPr, at 45 °C (8% conversion, three turnovers, based on the molar equivalents of V_6 groups in **4** present, after a reaction period of 7 days). In the absence of the catalytic microporous coordination polymer, no PrSSPr was produced (the limit of detectability is <0.1% conversion). In addition, the supernatant showed no catalytic activity. The FTIR spectrum of Co**4** before and after reaction was identical suggesting the material is completely stable under these reaction conditions. While the reaction is very slow, these results provide the proof of concept – a microporous coordination polymer ("metal organic framework") can be engineered to have a useful catalytic entity structurally incorporated in the wall of the pores. The linkages, counterions, and metal compositions in the esterified polyoxometalate units in Co**4**-like structures could all likely be altered synthetically so other crystalline microporous coordination polymeric materials capable of catalyzing air-based oxidations should be obtainable.

References

[1] C.L. Hill, C.M. Prosser-McCartha, Coord. Chem. Rev. 143 (1995) 407–455.
[2] G.-J. Brink, I.W.C.E. Arends, R.A. Sheldon, Science 287 (2000) 1636–1639.
[3] R.A. Sheldon, I.W.C.E. Arends, in: L.I. Simandi (Ed.), Advances in Catalytic Activation of Dioxygen by Metal Complexes, vol. 26, Kluwer, Dordrecht, 2003, pp. 123–156.
[4] E. Boring, Y.V. Geletii, C.L. Hill, J. Am. Chem. Soc. 123 (2001) 1625–1635.
[5] R. Ben-Daniel, P. Alsters, R. Neumann, J. Org. Chem. 66 (2001) 8650–8653.
[6] N.M. Okun, T.M. Anderson, C.L. Hill, J. Am. Chem. Soc. 125 (2003) 3194–3195.
[7] N.M. Okun, T.M. Anderson, K.I. Hardcastle, C.L. Hill, Inorg. Chem. 42 (2003) 6610–6612.
[8] T.M. Anderson, W.A. Neiwert, M.L. Kirk, P.M.B. Piccoli, A.J. Schultz, T. Koetzle, F.D.G. Musaev, K. Morokuma, R. Cao, C.L. Hill, Science 306 (2004) 2074–2077.
[9] N.M. Okun, J.C. Tarr, D.A. Hilleshiem, L. Zhang, K.I. Hardcastle, C.L. Hill, J. Mol. Catal. A: Chem 246 (2006) 11–17.
[10] R. Contant, Can. J. Chem. 65 (1987) 568–573.
[11] F. Zonnevijlle, C.M. Tourné, G.F. Tourné, Inorg. Chem. 21 (1982) 2751–2757.
[12] V.W. Day, W.G. Klemperer, D.J. Maltbie, J. Am. Chem. Soc. 109 (1987) 2991–3002.
[13] P.J. Domaille, in: A.P. Ginsberg (Ed.), Inorganic Syntheses, vol. 27, Wiley, New York, 1990, pp. 96–104.
[14] A.J.C. Wilson (Ed.), International Tables for X-ray Crystallography, vol. C, Kynoch, Academic Publishers, Dordrecht, 1992.
[15] Q. Chen, D.P. Goshorn, C.P. Scholes, X.L. Tan, J. Zubieta, J. Am. Chem. Soc. 114 (1992) 4667–4681.